19th Brazilian Congress of Thermal Sciences and Engineering
November 06th-10th, 2022, Bento Gonçalves - RS - Brazil

ENC-2022-0439
NUMERICAL SIMULATION OF TURBULENT COMPRESSIBLE FLOW OVER A SURFACE BUMP

Amanda Chenu Romano(1)
Carlos Henrique Melo Souza(1,2)
Danton José Fortes Villas Boas(2)
Humberto Araujo Machado(2,3)
Angelo Passaro(4)
(1) Instituto Tecnológico da Aeronáutica – ITA, Pç Mal. Eduardo Gomes 50, São José dos Campos, SP, 12228-900, Brazil
(2) Instituto de Aeronáutica e Espaço – IAE, Pç Mal. Eduardo Gomes 50, São José dos Campos, SP, 12228-904, Brazil
(3) Faculdade de Tecnologia – FAT/UERJ, Rod. Pres. Dutra km 298, Resende, RJ, 27537-000, Brazil
(4) Instituto de Estudos Avançados – IEAv, Trevo Cel. Av. José Alberto Albano do Amarante 01, Putim, São José dos Campos, SP, 12228-001, Brazil
amandaacr@ita.br, souzachms@fab.mil.br, dantondjfvb@fab.mil.br, humbertoham@fab.mil.br, angelo.passaro@pq.cnpq.br

Abstract. *Space and sub-orbital rockets reach high velocities in atmospheric flight, which results in compressible flows around their bodies. Diverse systems are placed in the external surface of such vehicles, appearing like bumps and disturbing the flow. The flow perturbation may result also in a wake formation afterward the bump. These effects affect the aerodynamic performance and the heat transfer in the surface and have to be accurate estimated in order to adjust the dynamic and thermal loads during the flight. In this work, a compressible turbulent flow over a bump is simulated and validated through the comparison with some literature results. Some turbulence models are applied in the simulation and compared with reference data, in order to evaluate their accuracy, allowing deciding the most adequate to this kind of problem.*

Keywords: *numerical simulation, turbulent flow, surface discontinuity*

1. INTRODUCTION

Vehicles in hypersonic flight are submitted to aerothermodynamic environments that impose significant thermal loads on the structure. These loads are developed by different processes of heat transfer that need to be previously analyzed through engineering models, wind tunnel tests or fluid dynamics computer programs. These last, when properly configured, provide reliable results with low error margins, emerging as a powerful tool in the aerothermodynamic analysis of space vehicles.

Although there is no point value of Mach number that ensures the hypersonic regime, it is possible to identify it through physical phenomena that become predominant. Among these phenomena can be highlighted strong shock waves with a significant entropy increase in the flow due to high velocities. Also, hypersonic flows are characterized by a large amount of kinetic energy, so part of the energy is converted into internal energy, leading to a local temperature increase.

Considering the phenomena mentioned above, the effect of protuberances on the external surfaces is prominent as those interfere with the free flow and result in three-dimensional interactions that increase the local heat flux. The heat increase on the vehicle surface is usually a topic of great concern in engineering designs, despite the possibility of building the protuberances with high-temperature resistant materials (Stollery, MacManus and Estruch, 2008). For this reason, experimental and numerical studies have been developed to understand the hypersonic effects better and identify the best configurations and techniques to control the characteristic phenomena of this flow regime.

Among the experimental studies developed in the area, Hung and Clauss (1980) and Hung and Patel (1984) investigated the flow separation induced by cylindrical and rectangular protuberances under laminar and turbulent regime conditions. These works show that the flow interactions induced by the presence of the protuberance depend not only on the geometry but also on the Reynolds number, the Mach number and the boundary layer regime. Since these factors influence the thermal properties in the vicinity of the protuberance, further experimental studies about their influences on the local heat transfer rate have been developed, as presented by Estruch et al. (2010) and Kumar and Reddy (2014).

Concerning research with computational tools, some studies using fluid dynamics programs were developed by Mazaheri and Wood (2009) after the Space Shuttle Columbia accident in 2003 to obtain a correlation for the heating increase on a repaired surface subjected to hypersonic flight. Despite this precedent and the increased access to commercial engineering software, the use of Computational Fluid Dynamics (CFD) programs for evaluating and studying thermal phenomena induced by protuberances in hypersonic flows remains a relatively unexplored field.

2. OBJECTIVE

The objective of this work was to compare the application of the k-ε, k-ω and Spalart-Allmaras turbulence models to predict the Stanton Number of the hot spot present at the front of protuberances in hypersonic speeds.

3. METHODOLOGY

The protuberances with inclination angles $\alpha = 45°$ and $\alpha = 60°$ that were used in the experiments of Estruch et al. (2010) were reproduced in two-dimensional models. The results presented and discussed in the reference work influenced the choice of those inclination angles since it shows that the flow upstream those is expected to separate, and so a hot spot will occur at these locations. High heat flux values upstream the protuberances are critical in the design of hypersonic vehicles (Estruch et al., 2010), which justified the interest in studying configurations like those.

Following the arrangement of the test model presented by Estruch et al. (2010), the domain made in CAD software for the protuberance with 45° is shown in Fig. 1. Further, for the protuberance with 60°, only the inclination angle was modified in the design. It should be noted that the total length of the domain is equal to the length of the plate used in the experimental tests, with the protuberance in just the proper position, to consider the entire boundary layer that develops at the plate before reaching it.

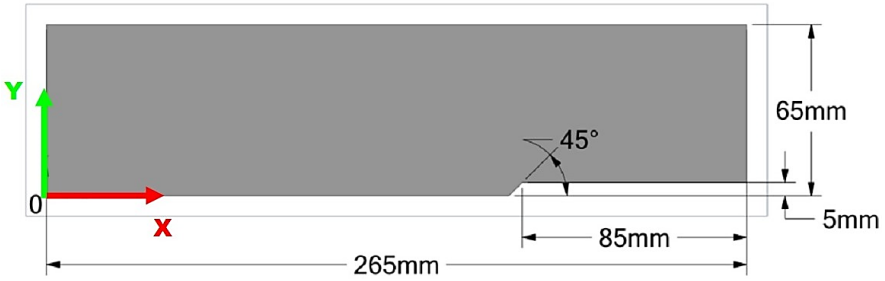

Figure 1. Geometric domain for protuberance with inclination angle $\alpha = 45°$.

To correctly capture the boundary layer in the simulations, 20 layers of quadrilateral elements with a growth rate of 1.1 were defined over the entire bottom length of the domain. In addition, for the regular mesh used in the simulations, the rest of the domain was discretized with elements of size 5 x 10^{-4} mm with the application of the quad/tri multizone method. Details of the mesh in the region of the protuberance with $\alpha = 45°$ can be seen in Fig. 2.

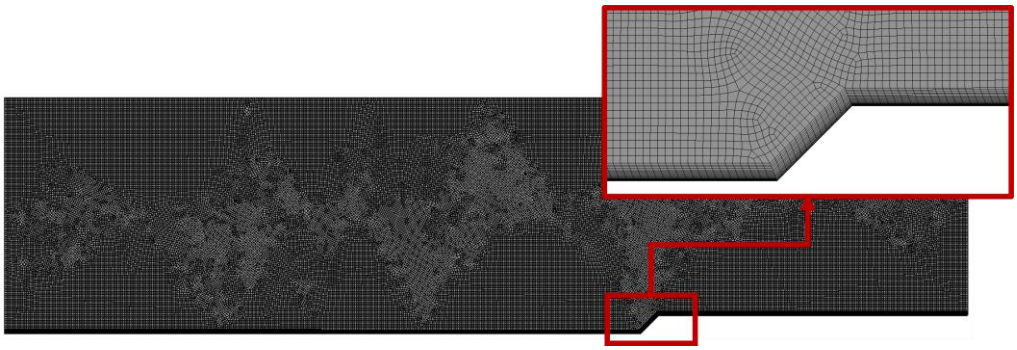

Figure 2. Mesh near the protuberance with inclination angle $\alpha = 45°$.

To perform a mesh convergence analysis the value of the Stanton Number obtained at position x = 0.174 mm for three meshes with different refinements was compared. In Tab. 1, it is possible to verify the variation of this parameter for the gross and the refined meshes to the regular mesh. The regular mesh was used for the simulations since the difference of the Stanton Number value to the most refined mesh is less than 1%, which was assumed to be satisfactory.

Table 1. Difference on Stanton Number at x = 174 mm for two meshes to the regular mesh.

Mesh	Elements Number	Stanton Number	Error
Gross mesh	54912	0.001695	4.54%
Regular mesh	76417	0.001776	-
Refined mesh	116958	0.001791	0.83%

Computational simulations were performed in Fluent® software, using the RANS (Reynolds Averaged Navier-Stokes) method, which solves averages of the Navier-Stokes equations, modeling all turbulence scales. The density-based solver was used, solving the equations of continuity, quantity of momentum, energy and species transport. In addition, the assumptions of two-dimensional flow, steady state, ideal gas and viscosity estimated by Sutherland's law (Sutherland, 1893) were considered.

A no-slip wall condition with a constant temperature of 295 K was established over the entire bottom length of the domain. Furthermore, at the other edges, the pressure far-field condition was established with the flow parallel to the x-axis, and the static pressure and temperature equivalent to the test data provided in the work of Estruch et al. (2010) for a Mach number equal to 8.2 and a Reynolds number of 9.35×10^6 in respect to the flat plate length.

In the solution methods, an implicit formulation was used to calculate convective fluxes using the AUSM (Advection Upstream Splitting Method), which belongs to the Flux-Vector Splitting Schemes and provides the exact solution at discontinuities such as shocks, being less susceptible to numerical instabilities. Regarding discretization, in all simulations, a second-order upwind scheme was used for all variables to achieve faster convergence. The simulations were performed for 10000 iterations, obtaining the convergence of the drag coefficient and the total heat transfer rate over the wall and an appropriate decrease of the residuals.

The difference between the simulations is set by the turbulence model employed. Between the RANS models with turbulent viscosity formulation provided in Fluent®, simulations were performed with the Spalart-Allmaras, k-ε and k-ω turbulence models. A brief review of them is presented below.

- **Spalart-Allmaras:** initially developed by Spalart and Allmaras (1992), the model adds to the original system of Navier-Stokes equations a single transport equation for a modified turbulent viscosity. This model is classified as a low Reynolds number model. It was developed for aerodynamic applications and provides good results for boundary layers subject to adverse pressure gradients. Finally, it can be pointed out that the Spalart-Allmaras model is relatively robust and has moderate requirements for its solution.

- **k-ε:** this model, whose formulation is presented by Launder and Spalding (1972), adds two transport equations to the original system of Navier-Stokes: one for the turbulent kinetic energy (k) and one for the dissipation rate of turbulent kinetic energy (ε). The k-ε model is popular in industrial applications due to its reasonable convergence rate and low memory usage. For the simulations performed in this work, the Realizable k-ε model was used, which constitutes a modification developed by Shih et al. (1995) in such a way that the model satisfies some mathematical constraints for Reynolds stresses, being consistent with the physics of turbulent flows. In addition, since the k-ε model is not classified as a low Reynolds number model, a wall treatment was employed. Among the options provided in Fluent®, the Enhanced Wall Treatment was used because it applies to flows with complex near-wall phenomena, such as pressure gradient and thermal effects.

- **k-ω:** the k-ω model, based on Wilcox (1998), adds to the original Navier-Stokes system two transport equations, one for the turbulent kinetic energy and one for the specific rate of dissipation of kinetic energy (ω). This model does not include undefined wall terms, so it is classified as a low Reynolds number model and does not require the use of wall functions. The k-ω model is extremely nonlinear, being more difficult to achieve convergence and more sensitive to initial conditions. For the simulations performed in this work, the SST (Shear Stress Transport) k-ω model, developed by Menter (1994), was chosen in Fluent®, because it uses a modified turbulent viscosity formulation to consider the transport effects of the main turbulent shear stress.

Considering the results of the CFD simulations, the primary analysis parameter was the Stanton Number (St), which represents the ratio of heat transfer coefficient to the heat capacity of the fluid. It can be estimated by Eq. (1), where q is the heat flux, ρ_∞ is the free flow's density, U_∞ is the free flow's velocity, c_p is the specific heat capacity at constant pressure and θ is the temperature relative to the wall.

$$St = \frac{q}{[\rho_\infty U_\infty c_p \theta]} \tag{1}$$

The adiabatic wall temperature was estimated to consistently compare the results obtained through the Fluent® simulations with those obtained in the experimental tests of Estruch et al. (2010), since θ is defined as the difference

between the adiabatic wall temperature and the wall temperature ($\theta = T_{aw} - T_w$). For this, Eq. (2) was used, in which T_∞ is the free flow's static temperature, γ is the ratio between the specific heats assumed to be 1.4 for air, r is the recovery coefficient considered to be the square root of Prandtl's number, which was assumed to be equal to 0.71, and M_∞ is the free flow's Mach number.

$$T_{aw} = T_\infty \left(1 + r\frac{\gamma-1}{2}{M_\infty}^2\right) \tag{2}$$

The estimated value of T_{aw} was used as the reference temperature for the software calculations, allowing the simulations performed to be coherence with the wind tunnel experiment, whose results were presented in the reference. Furthermore, comparisons were established not only with the Stanton Number obtained in the experimental tests but also with the result obtained by the application of the semi-empirical correlation established by Estruch et al. (2010), presented in Eq. (3), in which Re_h is the Reynolds number in relation to the height of the protuberance.

$$St_{max,ahead} = 5.2 \times 10^{-5} {Re_h}^{0.6} (1 - \cos\alpha) {M_\infty}^{-0.5} \pm 15\% \tag{3}$$

4. RESULTS

Figure 3 presents the values of the Stanton Number calculated through the CFD simulations in the vicinity of the protuberance with $\alpha = 45°$. The results shows that all the tested turbulence models estimated the highest value of St upstream the protuberance, which indicate that the simulations estimate the hot spot as well as the experimental tests whose results are presented in the reference. It can also be noted that the k-ω turbulence model provided the St highest values over the entire length upstream the protuberance and at the hot spot. Furthermore, it can be seen that the results of the k-ω turbulence model have similar behavior to the Spalart-Allmaras model, although this last one measures the hot spot St smallest value.

The Stanton Number results in the vicinity of the protuberance with $\alpha = 60°$ are displayed in Fig. 4. It can be seen that, when compared to the results presented in Fig. 3, the increase in the inclination angle led the k-ε model to estimate the St highest values in most regions upstream the protuberance, being this model the one that estimated the highest value at the hot spot. Also, it is observed again that the behavior of the k-ω and Spalart-Allmaras turbulence models are very similar and the Spalart-Allmaras model estimates the hot spot St lowest value.

Figure 5 presents the Stanton Number values measured for the hot spots through the turbulence models in comparison with the values found in the work of Estruch et al. (2010) and with those estimated through Eq. (3). It can be observed that with the increase of the inclination angle also increases the difference between the results. These statements lead to a belief that with the increase of the inclination angle, the phenomena related to the separation bubble upstream the protuberance and consequently to the hot spot at this location are more complex and could not be entirely captured by the simulations performed. It can also be seen in Fig. 5 that the k-ε model is most sensitive to the change in the inclination angle of the protuberance, followed by Spalart-Allmaras, while the k-ω model shows practically no variation.

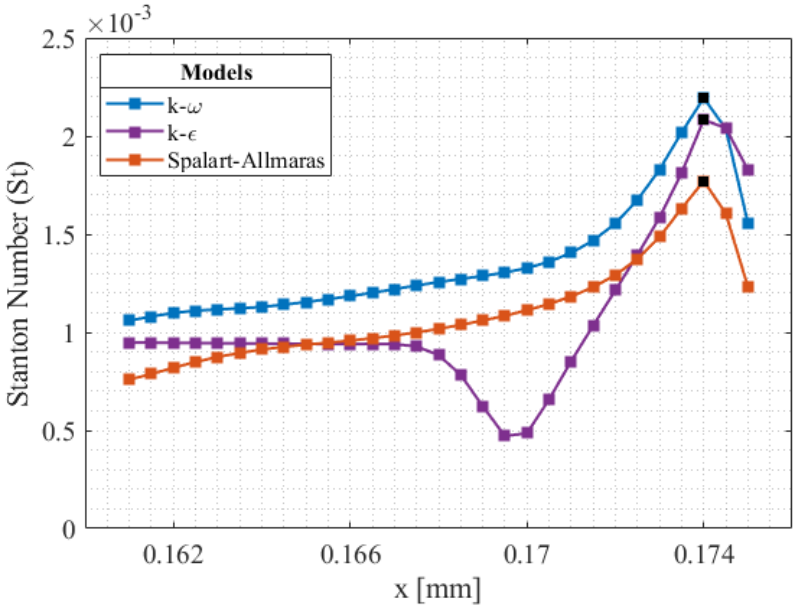

Figure 3. Stanton Number in the vicinity of the protuberance with α = 45°.

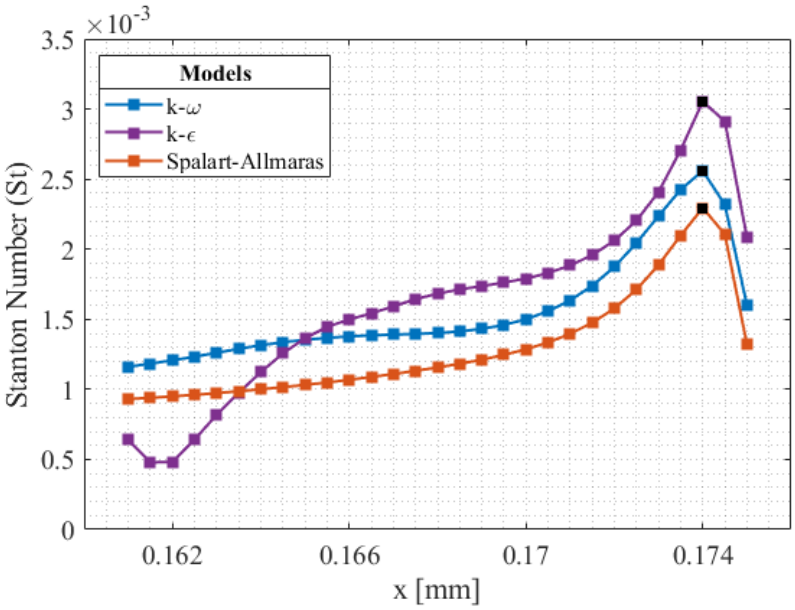

Figure 4. Stanton Number in the vicinity of the protuberance with α = 60°.

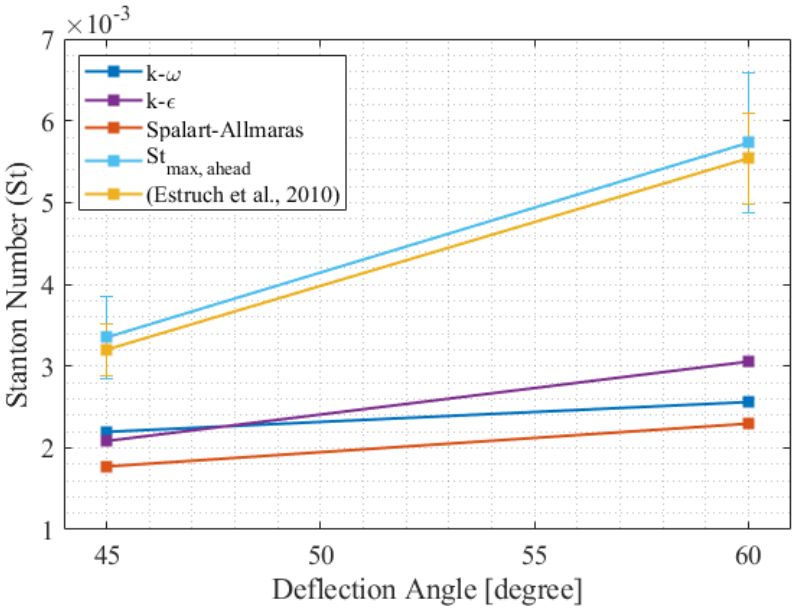

Figure 5. Stanton Number at hot spot as a function of deflection angle.

Table 2. Stanton numbers obtained from CFD simulations and relative errors for protuberance with α = 45°.

Model	Stanton Number	Error (Estruch el al., 2010)	Error (Eq. (3))
k-ω	0.00219	31%	34%
k-ε	0.00208	35%	37%
Spalart-Allmaras	0.00177	45%	46%

Table 3. Stanton numbers obtained from CFD simulations and relative errors for protuberance with α = 60°.

Model	Stanton Number	Error (Estruch el al., 2010)	Error (Eq. (3))
k-ω	0.00256	54%	55%
k-ε	0.00305	45%	47%
Spalart-Allmaras	0.00230	58%	60%

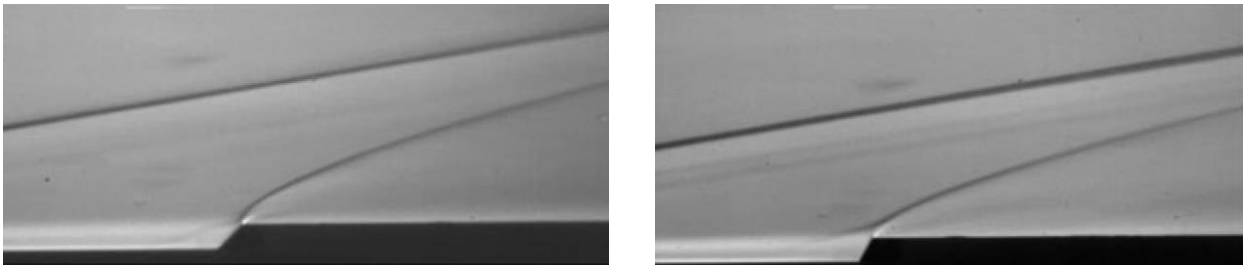

(a) Schlieren image (Estruch et al., 2010).

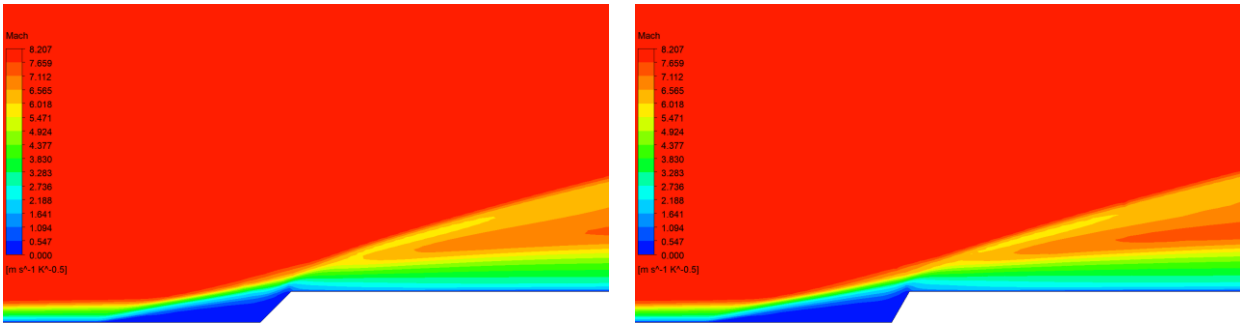

(b) Turbulence model: k-ω.

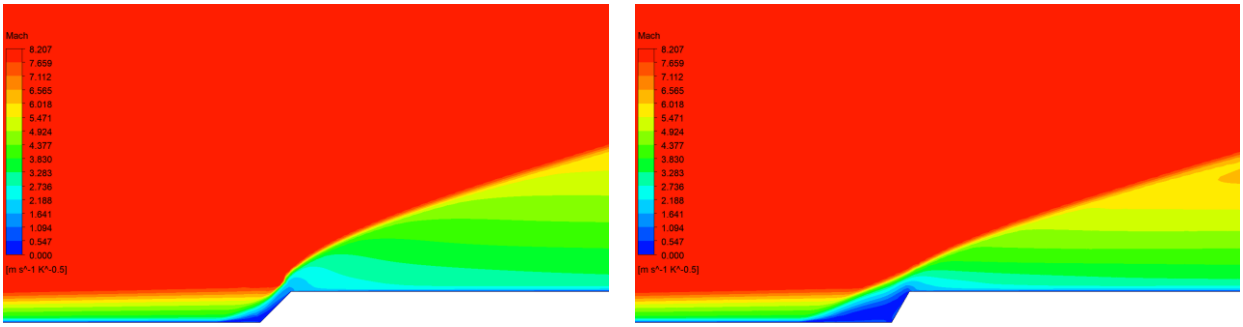

(c) Turbulence model: k-ε.

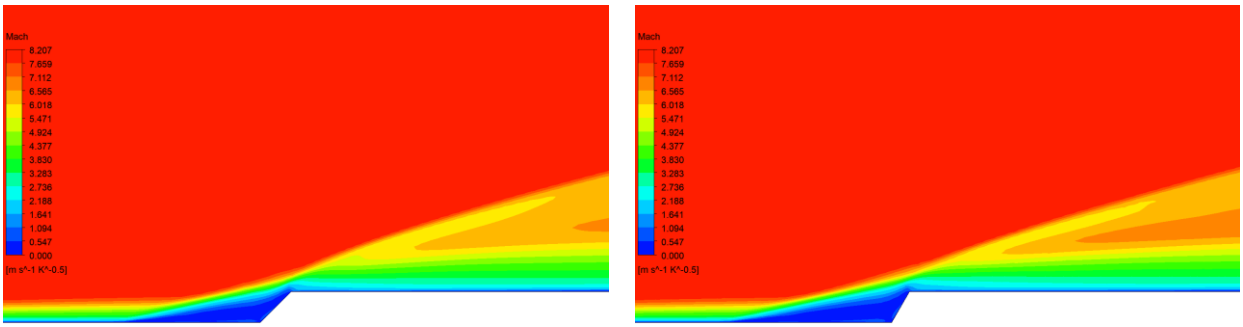

(d) Turbulence model: Spalart-Allmaras.

Figure 6. Mach number contours in the protuberance vicinity for inclination angles of α = 45° (left) and α = 60° (right).

Tabs.2,3 compare the highest Stanton Number values found in the CFD simulations with the values measured for the hot spot in the experimental tests performed by Estruch et al. (2010). It is possible to observe that the results from the computer simulations reach the same order as the experimental results, with differences in magnitude. Indeed, for $\alpha =$

45° the k-ω turbulence model, which estimated the highest value of St, achieves the magnitude closest to the expected one, while for $\alpha = 60°$ the best agreement between the results is obtained with the k-ε model.

The result obtained from the semi-empirical equation is higher than those found in the wind tunnel experiments and CFD simulations, leading to a higher relative error. A portion of this difference can be justified by the coefficient of Eq. (3), which was derived, according to Estruch et al. (2010), assuming a Prandtl number equal to 1. However, it was expected that the results of the CFD simulations would be closer to the tests and the estimated by Eq. (3), indicating that other solution methods could be explored for better capture the effects of surface interaction with hypersonic flow.

The Mach number contours in the region of the protuberance for each model simulated in CFD are shown in Fig. 6. It shows that the presence of the protuberance induces the formation of an attached shock, which was also evidenced in the Schlieren images presented in the work of Estruch et al. (2010). Through a visual comparison, it is suggested that the k-ε turbulence model better reproduces the formation of this shock wave.

All the turbulence models estimate the formation of a bounded boundary layer up to a region close to the protuberance, where the Spalart-Allmaras and k-ω models capture a significantly larger recirculation zone than the k-ε model. For k-ε model, the change of the protuberance inclination angle led to a more considerable difference in the capture of the separation, which is related to the Stanton number measured upstream the bump.

5. CONCLUSION

This work simulated and validated a compressible turbulent flow over a protuberance. The turbulence models Spalart-Allmaras, k-ε and k-ω are applied in the simulations and compared with reference data to evaluate their accuracy. The results show that all turbulence models tested could partially capture the interaction between the hypersonic flow and the bump. Furthermore, it has been demonstrated that the models provide a preliminary estimate of the thermal parameters with relative similarity to the values obtained in experimental tests.

6. ACKNOWLEDGEMENTS

This study was financed in part by the ***Coordenação de Aperfeiçoamento de Pessoal de Nível Superior – Brasil (CAPES)*** – Finance Code 001. This work was carried out with the support of the Academic Cooperation Program in National Defense (PROCAD-DEFENSE), grant 88881.387753/2019-01 and ***Conselho Nacional de Desenvolvimento Cientifico e Tecnológico (CNPq)*** under Grant 307691/2020-9.

7. REFERENCES

Estruch, D., MacManus, D., Stollery, J., Lawson, N. and Garry, K., 2010. “Hypersonic interference heating in the vicinity of surface protuberances”. *Experiments in Fluids*, 49(3), pp.683-699.

Hung, F. and Clauss, J., 1980. “Three-dimensional protuberance interference heating in high speed flow”. In *Proceedings of 18th Aerospace Sciences Meeting*.

Hung, F. and Patel, D., 1984. “Protuberance interference heating in high-speed flow”. In *Proceedings of 19th Thermophysics Conference.*

Kumar, C. and Reddy, K., 2014. “Hypersonic Interference Heating on Flat Plate with Short Three-Dimensional Protuberances”. *AIAA Journal*, 52(4), pp.747-756.

Launder, B. and Spalding, D., 1972. *Lectures in mathematical models of turbulence*. London: Acad. Pr.

Mazaheri, A. and Wood, W., 2009. Heating Augmentation for Short Hypersonic Protuberances. Journal of Spacecraft and Rockets, 46(2), pp.284-291.

Menter, F., 1994. “Two-equation eddy-viscosity turbulence models for engineering applications”. *AIAA Journal*, 32(8), pp.1598-1605.

Needham, D., 1963. *Progress report on the Imperial College hypersonic gun tunnel*.

Shih, T., Liou, W., Shabbir, A., Yang, Z. and Zhu, J., 1995. “A new k-ϵ eddy viscosity model for high reynolds number turbulent flows”. *Computers & Fluids*, 24(3), pp.227-238.

Spalart, P. and Allmaras, S., 1992. “A one-equation turbulence model for aerodynamic flows”. In *Proceedings of 30th Aerospace Sciences Meeting and Exhibit*.

Stollery, J., MacManus, D. and Estruch, D., 2008. *Hypersonic research and its application to a real vehicle*.

Sutherland, W., 1893. LII. “The viscosity of gases and molecular force”. *The London, Edinburgh, and Dublin Philosophical Magazine and Journal of Science*, 36(223), pp.507-531.

Wilcox, D., 1998. *Turbulence modeling for CFD*. La Canada, Calif.: DCW Industries.

8. RESPONSIBILITY NOTICE

The authors are the only responsible for the printed material included in this paper.